Neuropsychologia 63 (2014) 145–153

Contents lists available at ScienceDirect

Neuropsychologia

journal homepage: www.elsevier.com/locate/neuropsychologia

The steady-state visual evoked potential reveals neural correlates of the items encoded into visual working memory

Dwight J. Peterson [a,b,*], Gennadiy Gurariy [a], Gabriella G. Dimotsantos [a], Hector Arciniega [a], Marian E. Berryhill [a], Gideon P. Caplovitz [a]

[a] Program in Cognitive and Brain Sciences, Department of Psychology, University of Nevada, Reno, NV 89557, United States
[b] Department of Psychological Sciences, University of Missouri-Columbia, 9J McAlester Hall, Columbia, MO 65211-2500, United States

ARTICLE INFO

Article history:
Received 11 April 2014
Received in revised form
15 August 2014
Accepted 19 August 2014
Available online 28 August 2014

Keywords:
Visual working memory
Visual attention
Steady-state visual evoked potential

ABSTRACT

Visual working memory (VWM) capacity limitations are estimated to be ~4 items. Yet, it remains unclear why certain items from a given memory array may be successfully retrieved from VWM and others are lost. Existing measures of the neural correlates of VWM cannot address this question because they measure the aggregate processing of the entire stimulus array rather than neural signatures of individual items. Moreover, this cumulative processing is usually measured during the delay period, thereby reflecting the allocation of neural resources during VWM maintenance. Here, we use the steady-state visual evoked potential (SSVEP) to identify the neural correlates of individual stimuli at VWM encoding and test two distinct hypotheses: the *focused-resource* hypothesis and the *diffuse-resource* hypothesis, for how the allocation of neural resources during VWM encoding may contribute to VWM capacity limitations. First, we found that SSVEP amplitudes were larger for stimuli that were later remembered than for items that were subsequently forgotten. Second, this pattern generalized so that the SSVEP amplitudes were also larger for the unprobed stimuli in correct compared to incorrect trials. These data are consistent with the diffuse-resource view in which attentional resources are broadly allocated across the whole stimulus array. These results illustrate the important role encoding mechanisms play in limiting the capacity of VWM.

1. Introduction

The goal of the current experiment was to elucidate why we are able to retrieve certain items from visual working memory while others are forgotten. Visual working memory (VWM) refers to the encoding, maintenance, manipulation and retrieval of visual representations for immediate use. Despite the importance of VWM in both simple and complex cognitive tasks, capacity limitations associated with VWM are well documented (Cowan, 2001; Luck & Vogel, 2013). In addition, VWM capacity is further constrained by stimulus factors such as complexity (Alvarez & Cavanagh, 2004), saliency (Melcher & Piazza, 2011), similarity (Awh, Barton, & Vogel, 2007), and set size (Anderson, Vogel, & Awh, 2011; Bays & Husain, 2008; Bays, Catalao, & Husain, 2009; Fukuda, Awh, & Vogel, 2010). At a basic level, these capacity limitations indicate that when trying to encode, maintain, and retrieve a set of items in and from VWM, only a subset will ultimately be accessible. Although progress has been made in recent years, much remains unknown regarding the origins of this capacity limitation. In the current paper, we propose that constraints on capacity may manifest, in part, during the allocation of VWM resources at the time of encoding. We examine this hypothesis by examining neural signals associated with individual items during VWM encoding, and investigate whether modulations in these signals correlate with the success or failure of the corresponding item being subsequently retrieved from VWM.

Much of the existing research examining the neural correlates of VWM has focused on the delay-period or maintenance-phase of VWM tasks. Electrophysiological and neuroimaging findings indicate that VWM is mediated in part by elevated and sustained neural activity during the delay-period of VWM tasks. Evidence in support of this view emerged from electrophysiological recordings from the prefrontal cortex (PFC) of nonhuman primates. PFC neurons increase firing rates during stimulus presentation and maintain elevated firing rates during the VWM maintenance period of delayed response tasks (e.g., Fuster & Alexander, 1971; Funahashi, Bruce, & Goldman-Rakic, 1990). Neuroimaging studies in humans have identified sustained neural activity during the

* Corresponding author at: Department of Psychological Sciences, University of Missouri-Columbia, 9J McAlester Hall, Columbia, MO 65211-2500, United States. Tel.: +1 573 882 8123.
E-mail address: petersondj@missouri.edu (D.J. Peterson).

http://dx.doi.org/10.1016/j.neuropsychologia.2014.08.020
0028-3932/

delay-period of VWM tasks (fMRI: Magen, Emmanouil, McMains, Kastner, & Treisman, 2009; Todd & Marois, 2004; Xu & Chun, 2006); event-related potentials (ERP: Vogel & Machizawa, 2004; Vogel, McCollough, & Machizawa, 2005). Moreover, in regions such as the intraparietal sulcus, the magnitude of the delay-period activity increases parametrically with set size (Todd & Marois, 2004; Xu & Chun, 2006) and asymptotes at an individual's VWM capacity limit (Todd & Marois, 2005). Similarly, ERP studies deriving the contralateral delay activity (CDA) from posterior electrode sites show sustained maintenance-phase activity that parametrically varies in amplitude with set size and asymptotes as capacity limits are reached (Vogel & Machizawa, 2004). These converging patterns of evidence are consistent with neural models of VWM that emphasize the importance of sustained maintenance-related patterns of elevated activity within posterior parietal cortex (PPC) and PFC regions. Moreover, these perspectives implicitly and explicitly suggest that the VWM capacity limitation arises due to these maintenance-phase processes.

An alternative view of VWM is sometimes termed the *sensory-recruitment* model of VWM (Awh & Jonides, 2001; D'Esposito, 2007; Postle, 2006). This view is derived from a recent wealth of evidence that cortical regions involved during perception are reactivated to aid in the storage and retrieval of stimuli encoded into VWM (e.g., (Albers, Kok, Toni, Dijkerman, & de Lange, 2013; Ester, Serences, & Awh, 2009; Emrich, Riggall, LaRocque, & Postle, 2013; Ester, Anderson, Serences, & Awh, 2013; Harrison & Tong, 2009; Serences, Ester, Vogel, & Awh, 2009). To examine the sensory-recruitment perspective, recent fMRI experiments have leveraged univariate and multivariate (multivoxel pattern analysis, MVPA) techniques to measure BOLD responses and decode sub-threshold activation patterns to improve our understanding of the mechanisms underlying VWM. Even in the absence of sustained, elevated patterns of maintenance-related activity in visual cortex (e.g., V1–V4, hMT+), decoding procedures reveal that the same sensory regions (e.g., V1–V4, hMT+) that are initially engaged in stimulus perception are involved in storing representations of those task relevant features during the delay-period of VWM tasks (Ester et al., 2009; Emrich et al., 2013; Ester et al., 2013; Harrison & Tong, 2009; Offen, Schuppeck, & Heeger, 2009; Riggall & Postle, 2012; Serences et al., 2009). In addition to the role of early visual regions, intermediate dorsal (V3a/b) and ventral (LO1/2) visual areas become significantly more active when engaged in effortful VWM encoding (Sneve, Alnaes, Endestad, Greenlee, & Magnussen, 2012). Thus, according to this view, limitations in VWM capacity may arise due to the inability to reactivate and maintain the perceptual representations of the multiple items present in the stimulus display. Experiments examining the *sensory-recruitment* model largely focus on the maintenance phase of VWM tasks. However, to maintain a representation of a stimulus in VWM it must first be encoded. As such, capacity limitations that arise during encoding may become apparent during the maintenance phase and contribute in general to the overall capacity limitation of VWM.

Several studies have examined the correspondence between encoding and maintenance related VWM activity within both visual cortex and higher-order regions of the brain. Successful encoding and maintenance of visual information relies on intracortical communication (e.g., Fuster, Bauer, & Jervey, 1985; Gazzaley, Rissman, & D'Esposito, 2004; McIntosh, Grady, Haxby, Ungerleider, & Horwitz, 1996). Recent fMRI evidence shows that greater correspondence in neural activity between encoding and maintenance processes in cortical regions (e.g., lateral PFC) is associated with successful VWM performance (Cohen, Sreenivasan, & D'Esposito, 2012). Importantly, enhanced functional connectivity between the lateral PFC and extrastriate cortex (EC) during VWM encoding and maintenance is associated with successful VWM performance (Cohen et al., 2012). These findings further stress the importance of accurate perceptual representations and successful encoding of the items to be maintained in and retrieved from VWM. Any limitation in the capacity to represent and encode the to-be-retrieved items will necessarily contribute to the overall capacity limitation of VWM.

In the current investigation of VWM, we were concerned with the fundamental question of why certain stimulus items are selected and subsequently retrieved from VWM while others are forgotten. This selection process must begin during encoding and impose a fundamental limitation in our ability to subsequently maintain and successfully retrieve information from VWM. The experiment described below reveals that neural processing associated with the encoding of a specific item in a VWM display can indeed influence whether or not that item will be subsequently retrieved. Moreover, the experiment tests two alternative hypotheses for how and why some items are successfully encoded while others may not be (Fig. 1A). First, participants may deliberately attempt to encode only a subset of items in a given memory array. This could happen, for example, if participants selectively allocate attentional resources to a subset of items in the display. We term this the *focused-resource* hypothesis. It predicts that if one of the items from the encoded subset is later probed, attempts at retrieval will be successful, but if the probed item was not in the subset at encoding, a retrieval failure will occur. The intuition behind this hypothesis is similar to the notion that providing a predictive attentional pre-cue would facilitate the VWM encoding, maintenance, and retrieval of the cued item. In this case, one may predict that neural signatures at the time of encoding of probed items successfully retrieved from working memory will be greater than those that are forgotten. In contrast, neural signatures of unprobed items would be expected to be greater on trials in which the probed item was forgotten than when it was successfully retrieved (Fig. 1A).

Alternatively, it may be the case that observers attempt to encode all of the items in a VWM display, but on a trial-by-trial basis they will not always succeed. This *diffuse-resource* hypothesis proposes that participants try to encode all items, but sometimes, due to distraction, lower motivation, or fluctuation in the overall amount of available attentional resources on a given trial, VWM performance suffers. According to this hypothesis, neural signals of both probed and unprobed items should be greater when the probed item is subsequently remembered than when it is forgotten (Fig. 1B).

We investigated these hypotheses using the steady-state visual evoked potential (SSVEP: Regan, 1989). The SSVEP is an electrophysiological signal derived from the EEG in response to temporally-periodic stimuli (i.e., stimuli flickering at a specific rate). In research investigating human cognition (e.g., visual attention), the SSVEP has been most commonly considered in the frequency domain and is used specifically when analyzing signal power in the EEG at frequencies associated with the flicker rates of experimental stimuli (Appelbaum & Norcia, 2009; Hillyard et al. 1997; Morgan, Hansen, & Hillyard, 1996; Muller et al. 1998; Muller & Hubner, 2002). One simple way to conceptualize the SSVEP is that a flickering stimulus will produce an EEG signal with increased power at the flicker frequency and/or one of its harmonics.

In the current experiment, we investigated the hypotheses described above by examining SSVEPs in response to the items present at the encoding phase of a VWM change detection task. This was accomplished by having the to-be-remembered items flicker at unique frequencies (3 Hz, 5 Hz, 12 Hz, 20 Hz). This allowed us to examine power in the SSVEP at frequencies corresponding to each item ($1f_1$=3 Hz; $1f_2$=5 Hz, $1f_3$=12 Hz, $1f_4$=20 Hz) and their second harmonics ($2f_1$=6 Hz, $2f_2$=10 Hz,

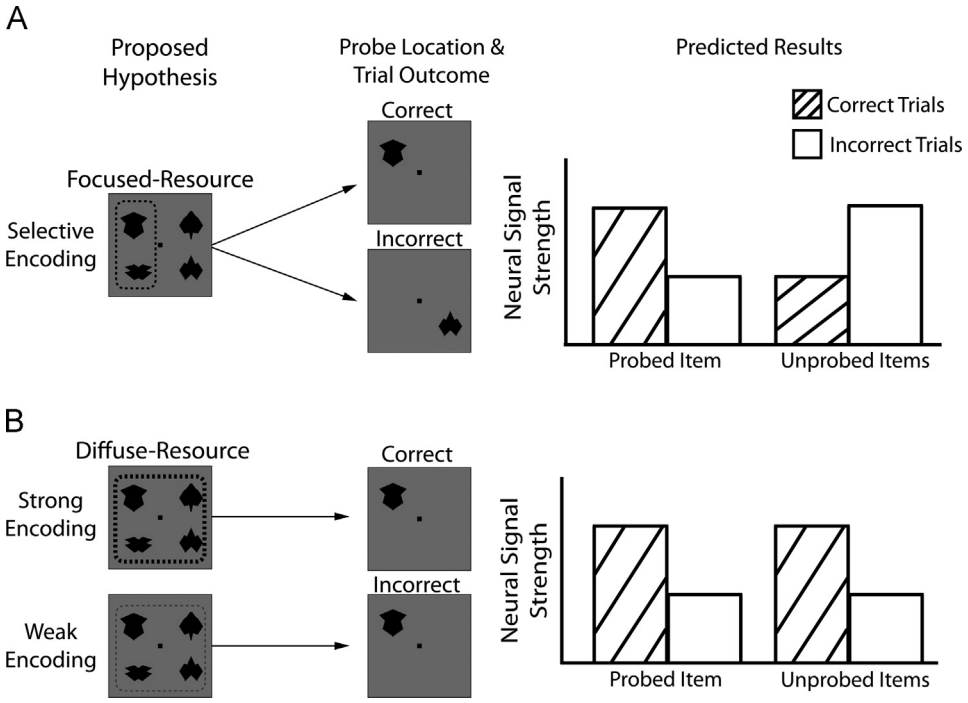

Fig. 1. Hypotheses related to the deployment of VWM resources during encoding. Schematic depictions of our predictions regarding two possible routes for the deployment of neural resources during VWM encoding. (A) According to the focused-resource hypothesis, encoding resources are deployed to a subset of the items within the memory array. (B) In contrast, the diffuse-resource hypothesis predicts that VWM resources are distributed across all of the items in the array during encoding. Each of these hypotheses predicts a different pattern of encoding-related neural activity during correct compared to incorrect trials for both the probed and unprobed items within the memory array.

$2f_3 = 24$ Hz, $2f_4 = 40$ Hz) independently (e.g., see Fig. 2) and sort the data according to whether a given stimulus was later probed or unprobed and whether or not the probed item was successfully retrieved from VWM. As described above, the hypotheses discussed above make specific predictions about how the SSVEP may reflect neural processes and their capacity limitations, operating at the encoding stage of VWM. In the following sections, we describe this novel approach for studying encoding in detail and interpret the findings in terms of the role that perceptual and cognitive processes (e.g., attention) may play in determining which items are successfully encoded into VWM.

2. Materials and methods

2.1. Participants

Twenty-three, right-handed, neurologically normal adults with normal or corrected-to-normal visual acuity participated in the current experiment (14 female, mean age: 24). The Institutional Review Board at the University of Nevada, Reno approved all experimental protocols and participants provided written informed consent.

2.2. Stimulus presentation

Stimuli were displayed on a 120-Hz CRT monitor (Dell Trinitron P991, 19 in., 1024×768) running via a 2.6 MHz MacMini and were presented using the Psychophysics Toolbox (Brainard, 1997; Pelli, 1997) for MATLAB (MathWorks Inc., Natick, MA). Each participant viewed the stimuli from a distance of 57 cm.

2.3. Electrophysiological recordings

The electroencephalogram (EEG) was collected from seven sites: O1, O2, Oz, P1, P2, C1, C2 (referenced to Fz, grounded to the forehead) according to the standard 10/20 electrode system (Jasper, 1958; Klem, Luders, Jasper, & Elger, 1999) using Grass Instruments® Ag/Ag electrodes. Electrode impedance was kept below 5 kΩ at 30 Hz. The EEG was amplified using an SA Instruments® Bio Amplifier with a gain factor of 50 K and bandpass analog filter of 0.3–500 Hz. The amplified signal was digitized using an eight channel Swissonic AD24 24-bit analog to digital converter with a sampling rate of 48 kHz per channel. The digital data were recorded using the Audacity® software package running on a 2.6 MHz MacMini workstation. A photodiode was attached to the CRT monitor and used to temporally synchronize the stimulus presentation onset with the recorded EEG. Photodiode output was amplified using a transimpedance amplifier and digitized with the EEG data via one channel of the AD converter.

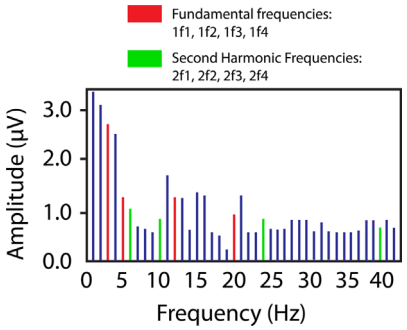

Fig. 2. Fundamental and second harmonic frequencies of interest. Fundamental (red) and second harmonic frequencies (green) of interest that were detectable from the SSVEP in the current experiment. The *y*-axis depicts the amplitude scale (microvolts) of the SSVEP. The *x*-axis depicts a subset of the fundamental and second harmonic frequencies (Hz) that were detectable from the SSVEP. (For interpretation of the references to color in this figure legend, the reader is referred to the web version of this article.)

2.4. Experimental procedure

Participants performed a VWM change detection task with a set size of four items, see Fig. 3. Trials began with a black central fixation point ($0.35^\circ \times 0.35^\circ$) on a neutral gray background (500 ms). Next, four shapes (randomly selected without replacement from a set of ten) were presented (1000 ms). Stimuli were bilaterally symmetrical abstract shapes ($7^\circ \times 7^\circ$) generated by a computer algorithm described previously (e.g., (Berryhill & Olson, 2008; Jiang, Olson, & Chun, 2000). Each shape reversed contrast (black, white) at one of four distinct temporal frequencies: 3 Hz, 5 Hz, 12 Hz, and 20 Hz. Thus, a shape flickering at 20 Hz would reverse contrast

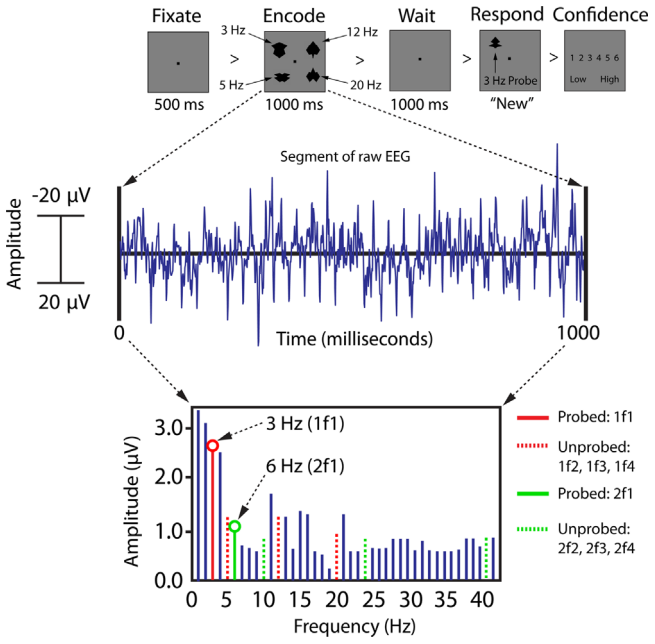

Fig. 3. Visual working memory task and data processing sequence. The visual working memory change-detection task and data processing sequence for each trial used in the current experiment. Participants viewed a fixation cross (500 ms), followed by a memory array (1000 ms) in which each item flickered at a distinct frequency (3 Hz, 5 Hz, 12 Hz, and 20 Hz). Following stimulus presentation, a delay period occurred. Finally, a single static probe stimulus appeared in one of the previously presented locations and remained until the participant decided whether it matched the stimulus shape presented in that location in the memory array by pressing the "o" (old) or "n" (new) key. Participants rated their confidence in their decision on each trial using a Likert-type scale ranging from 1 (low confidence) to 6 (high confidence). Epochs time-locked to the onset of the stimulus array (1000 ms in duration), were extracted from the unfiltered, continuous EEG. A Fourier transform was then applied to each epoch such that the SSVEP amplitudes of the fundamental (red) and second order harmonic (green) frequencies, corresponding to each item in the memory array (probed: solid lines; unprobed: dashed lines), could be measured. A 3-Hz correct trial in which the probed stimulus, previously flickering at 3-Hz during encoding, changed shape from sample to test and the participant responded "new" is depicted. (For interpretation of the references to color in this figure legend, the reader is referred to the web version of this article.)

every 25 ms. Each shape was presented within one of the four quadrants of the visual field. The locations of stimuli within each quadrant were randomly determined (potential jitter of 1–3° from each quadrant center). Stimulus flicker frequencies and shapes were randomized with respect to stimulus location. In other words, any shape could have been presented in any of the four quadrants and could have flickered at any of the four stimulus frequencies on any given trial.

Frequencies of 3 Hz, 5 Hz, 12 Hz, and 20 Hz were chosen because stimulus duration (1000 ms) allowed for exact periods of stimulation using a 120 Hz frame refresh rate on the CRT monitor. In addition, this approach allowed linearly independent frequencies for each stimulus to be recorded up to and including the 3rd harmonic of each fundamental frequency. Stimulus offset was followed by a VWM delay period (1000 ms). At test, a single, static probe image appeared at a previously occupied location. Participants responded using their right ring finger to press the "o" key if the item in the probed location was old or their right index finger to press the "n" key if the item was new. For old trials (50% of trials), the shape presented in the probed location did not change from sample to test. For new trials (50% of trials), the shape presented in the probed location changed from sample to test. Finally, participants made confidence judgments regarding their response using a Likert-type scale ranging from 1 (low confidence) to 6 (high confidence). A blank inter-stimulus interval varying in duration (1000–1500 ms) followed each confidence judgment. Participants were instructed to maintain central fixation throughout the trial with explicit instruction to not blink or break fixation while stimuli were on the screen (i.e., the encoding phase).

Prior to the experiment, participants completed 20 practice trials to familiarize themselves with the change detection task. Each participant completed the experiment in 10 separate blocks consisting of 40 trials per block for a total of 400 randomized trials such that an equal number of probed locations corresponded to each stimulus flicker rate (i.e., the location of the 20 Hz stimulus was probed 100 total times: 50 on new trials and 50 on old trials). At the end of each block, participants were prompted to take a break, prior to continuing on to the next block of trials.

2.5. Electrophysiological data processing and analysis

The digitized EEG data for all 23 participants were processed and analyzed using custom scripts written in MATLAB. Data from each channel were first downsampled from 48 kHz to 1000 Hz. Four hundred epochs, time-locked to the onset of the stimulus array (1000 ms in duration), were extracted from the unfiltered, continuous EEG. A Fourier transform was then applied to each epoch so that the SSVEP amplitudes of the fundamental and second order harmonic frequencies, corresponding to each item in the memory array, could be measured; see Fig. 3. Individual trials were then sorted according to trial accuracy and the flicker frequency of the to-be-probed item (3 Hz-correct, 3 Hz-incorrect, 5 Hz-correct, 5 Hz-incorrect, 12 Hz-correct, 12 Hz-incorrect, 20 Hz-correct, 20 Hz-incorrect). Event-related averages and amplitude spectra were computed for each condition.

Given the relatively high VWM accuracy across participants ($M=0.78$), there were many more correct than incorrect trials. To ensure fair comparisons using an equal number of epochs, average responses were computed on the basis of the smaller number of incorrect responses. This was done independently for each participant and each frequency through permutation analysis. A random subset of correct trials was selected that equaled the number of incorrect trials (e.g., if there were only 30 incorrect and 70 correct trials in the 3 Hz condition, 30 of the 70 were picked during each permutation). The amplitude spectrum was then computed based on this average. To avoid the random selection of an outlier subset of trials, this permutation test process was repeated 100,000 times.

For each condition the amplitudes of the fundamental frequencies "1*f*" (i.e., 3, 5, 12, 20 Hz) and second harmonics "2*f*" (i.e., 6, 10, 24, 40 Hz) were extracted from the amplitude spectrum. For example, for correct and incorrect trials in which the probed item initially flickered at 3 Hz during encoding, the 3 Hz ($1f_1$) and 6 Hz ($2f_1$) amplitudes were used to index neural activity related to the encoding of the probed item. The amplitudes of the "unprobed" frequencies 5 Hz, 12 Hz, 20 Hz ($1f_2$, $1f_3$, $1f_4$) and their second harmonics ($2f_2$, $2f_3$, $2f_4$) were used to index neural activity related to the encoding of the unprobed items. Given that the power of the SSVEP signal decreases at higher frequencies (e.g., 20 Hz compared to 3 Hz), for each condition we normalized the SSVEP amplitudes across our stimulus frequencies of interest for correct and incorrect trials and averaged across the four frequencies for both the fundamental (1*f*) and second harmonic (2*f*) frequency using the formulas:

$$\text{Correct}_{1f_{\text{probed}}} = \frac{1}{4}\sum_{i=1}^{4}\frac{1fi_{\text{probed}}\text{correct}}{1fi_{\text{probed}}\text{correct} + 1fi_{\text{probed}}\text{incorrect}}$$

$$\text{Incorrect}_{1f_{\text{probed}}} = \frac{1}{4}\sum_{i=1}^{4}\frac{1fi_{\text{probed}}\text{incorrect}}{1fi_{\text{probed}}\text{correct} + 1fi_{\text{probed}}\text{incorrect}}$$

$$\text{Correct}_{2f_{\text{probed}}} = \frac{1}{4}\sum_{i=1}^{4}\frac{2fi_{probed}correct}{2fi_{\text{probed}}\text{correct} + 2fi_{\text{probed}}\text{incorrect}}$$

$$\text{Incorrect}_{2f_{\text{probed}}} = \frac{1}{4}\sum_{i=1}^{4}\frac{2fi_{\text{probed}}\text{incorrect}}{2fi_{\text{probed}}\text{correct} + 2fi_{\text{probed}}\text{incorrect}}$$

We used the same basic formulas to compute normalized SSVEP amplitudes for the unprobed items. However, for each frequency of the probed item, there are three corresponding unprobed frequencies. Thus, the normalized SSVEP amplitudes for the corresponding unprobed items were based on the average amplitudes of these three remaining unprobed frequencies. For example, on trials in which the 3 Hz item was later probed, the stimuli that flickered at 5 Hz, 12 Hz, and 20 Hz would be considered "unprobed" items, thus:

$$\text{Correct}_{1f_{\text{unprobed}}} = \frac{1}{4}\sum_{i=1}^{4}\frac{1fi_{\text{unprobed}}\text{correct}}{1fi_{\text{unprobed}}\text{correct} + 1fi_{\text{unprobed}}\text{incorrect}}$$

$$\text{Incorrect}_{1f_{\text{unprobed}}} = \frac{1}{4}\sum_{i=1}^{4}\frac{1fi_{\text{unprobed}}\text{incorrect}}{1fi_{\text{unprobed}}\text{correct} + 1fi_{\text{unprobed}}\text{incorrect}}$$

$$\text{Correct}_{2f_{\text{unprobed}}} = \frac{1}{4}\sum_{i=1}^{4}\frac{2fi_{\text{unprobed}}\text{correct}}{2fi_{\text{unprobed}}\text{correct} + 2fi_{\text{unprobed}}\text{incorrect}}$$

$$\text{Incorrect}_{2f_{\text{unprobed}}} = \frac{1}{4}\sum_{i=1}^{4}\frac{2fi_{\text{unprobed}}\text{incorrect}}{2fi_{\text{unprobed}}\text{correct} + 2fi_{\text{unprobed}}\text{incorrect}}$$

where

$$1fi_{\text{unprobed}} = \frac{1}{3}\sum_{j=\{1\,2\,3\,4\}\setminus i} 1fj$$

$$2fi_{\text{unprobed}} = \frac{1}{3}\sum_{j=\{1\,2\,3\,4\}\setminus i} 2fj$$

As such, for each participant, 28 values were computed for the fundamental frequency and second harmonic: 2 accuracy: correct and incorrect; × 2 probe status: probed and unprobed; × 7 electrode: O1, O2, Oz, P1, P2, C1, C2.

3. Results

3.1. Behavioral accuracy

First, we tested whether flicker frequency influenced performance. The mean accuracy (proportion of correct trials) across all participants collapsed across the four frequencies was $M=0.78$. Performance did not significantly vary as a function of probed frequency (Means: 3 Hz: 0.78; 5 Hz: 0.81; 12 Hz: 0.77; 20 Hz: 0.78), single factor repeated-measures ANOVA ($F(3,66)=2.48$, $p=0.07$). Unfortunately, because there were too few low confidence trials per frequency we were unable to conduct analyses incorporating confidence judgments.

3.2. SSVEP amplitude as a function of VWM accuracy and probe status

Across all electrodes the mean normalized SSVEP amplitude values (see Table 1 and Fig. 4) corresponding to the fundamental frequency (e.g., 3 Hz, 5 Hz, 12 Hz, 20 Hz) of the probed items were larger for correct compared to incorrect trials. This was true for both probed and unprobed items. The statistical significance of these results was analyzed with a $2\times2\times7$ repeated measures ANOVA including the factors of accuracy (correct and incorrect), probe status (probed and unprobed), and electrode site (O1, O2, Oz, P1, P2, C1, C2). The main effect of accuracy approached significance ($F(1,22)=3.99$, $MSE=0.13$, $p=0.058$, $\eta_p^2=0.15$); however, no other main effects or interactions between any of the three factors included in the ANOVA were significant. We note that the formula used to normalize the SSVEP amplitudes across frequency precludes analysis of the main effect of probe status or the interaction between electrode and probe status.

The analysis of the SSVEP amplitudes corresponding to the second harmonic (e.g., 6 Hz, 10 Hz, 24 Hz, 40 Hz) revealed the same general pattern just described, but to a greater degree; see Table 2 and Fig. 5. Again, across all electrodes the mean normalized SSVEP amplitudes were greater for the correct than incorrect trials. This was the case for both the probed and unprobed items.

Table 1
Mean normalized SSVEP amplitudes by accuracy and probe type (1f).

Electrode	Correct probed	Incorrect probed	Correct unprobed	Incorrect unprobed
O1	0.51 (0.01)	0.49 (0.01)	0.51 (0.007)	0.49 (0.007)
O2	0.51 (0.01)	0.49 (0.01)	0.50 (0.006)	0.50 (0.006)
Oz	0.51 (0.01)	0.49 (0.01)	0.51 (0.007)	0.49 (0.007)
P1	0.52 (0.02)	0.48 (0.02)	0.51 (0.008)	0.49 (0.008)
P2	0.52 (0.02)	0.48 (0.02)	0.51 (0.007)	0.49 (0.007)
C1	0.54 (0.02)	0.46 (0.02)	0.52 (0.01)	0.48 (0.01)
C2	0.53 (0.02)	0.47 (0.02)	0.51 (0.009)	0.49 (0.009)

Table 2
Mean normalized SSVEP amplitudes by accuracy and probe type (2f).

Electrode	Correct probed	Incorrect probed	Correct unprobed	Incorrect unprobed
O1	0.53 (0.02)	0.47 (0.02)	0.51 (0.009)	0.49 (0.009)
O2	0.52 (0.01)	0.48 (0.01)	0.51 (0.009)	0.49 (0.009)
Oz	0.53 (0.01)	0.47 (0.01)	0.51 (0.01)	0.49 (0.01)
P1	0.53 (0.02)	0.47 (0.02)	0.52 (0.01)	0.48 (0.01)
P2	0.52 (0.02)	0.48 (0.02)	0.51 (0.009)	0.49 (0.009)
C1	0.53 (0.01)	0.47 (0.01)	0.52 (0.009)	0.48 (0.009)
C2	0.54 (0.02)	0.46 (0.02)	0.52 (0.009)	0.48 (0.009)

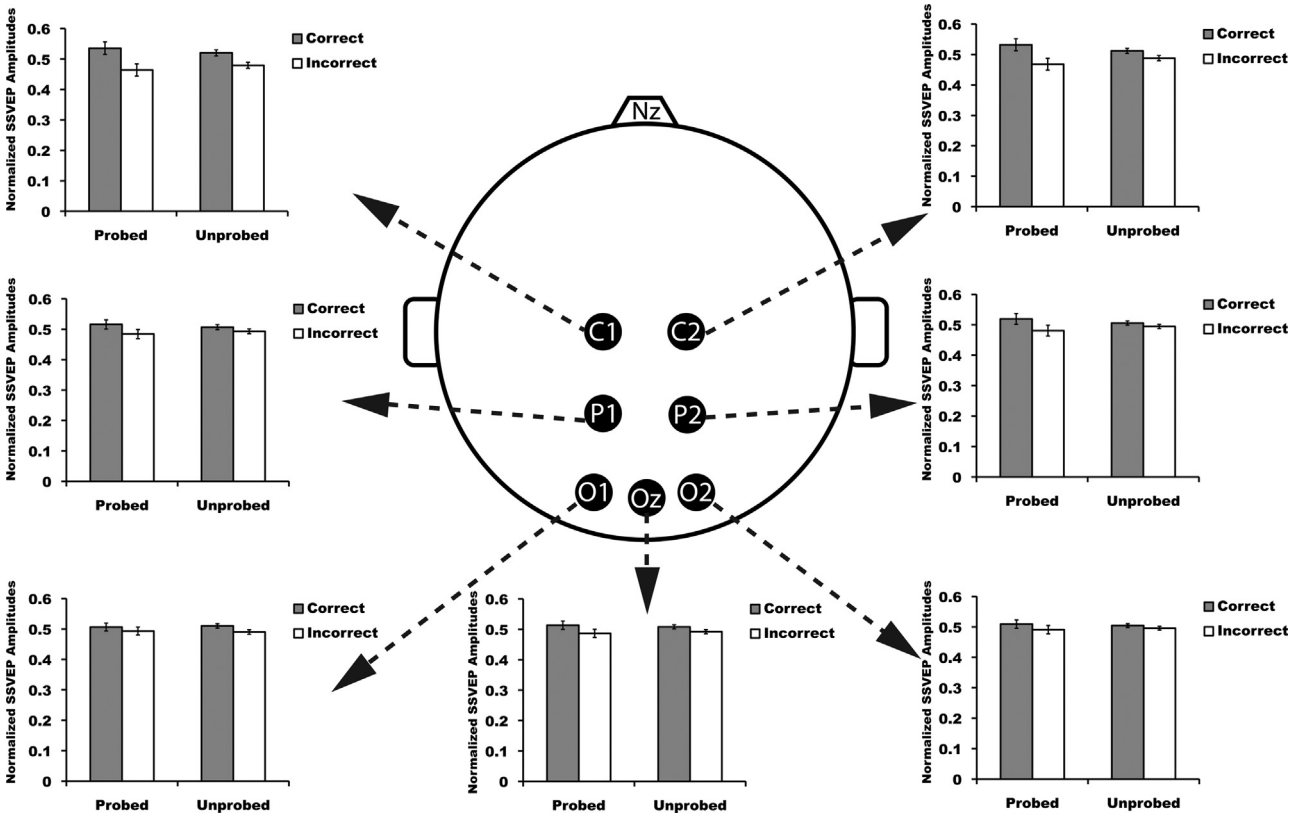

Fig. 4. SSVEP amplitudes as a function of accuracy and probe status at each electrode. SSVEP amplitudes for the fundamental frequencies (1f) computed from the steady-state visual evoked potentials corresponding to electrode sites O1, O2, Oz, P1, P2, C1, and C2. The *y*-axes indicate the mean normalized SSVEP amplitudes for the fundamental frequencies (1f). Error bars represent the standard errors of the means.

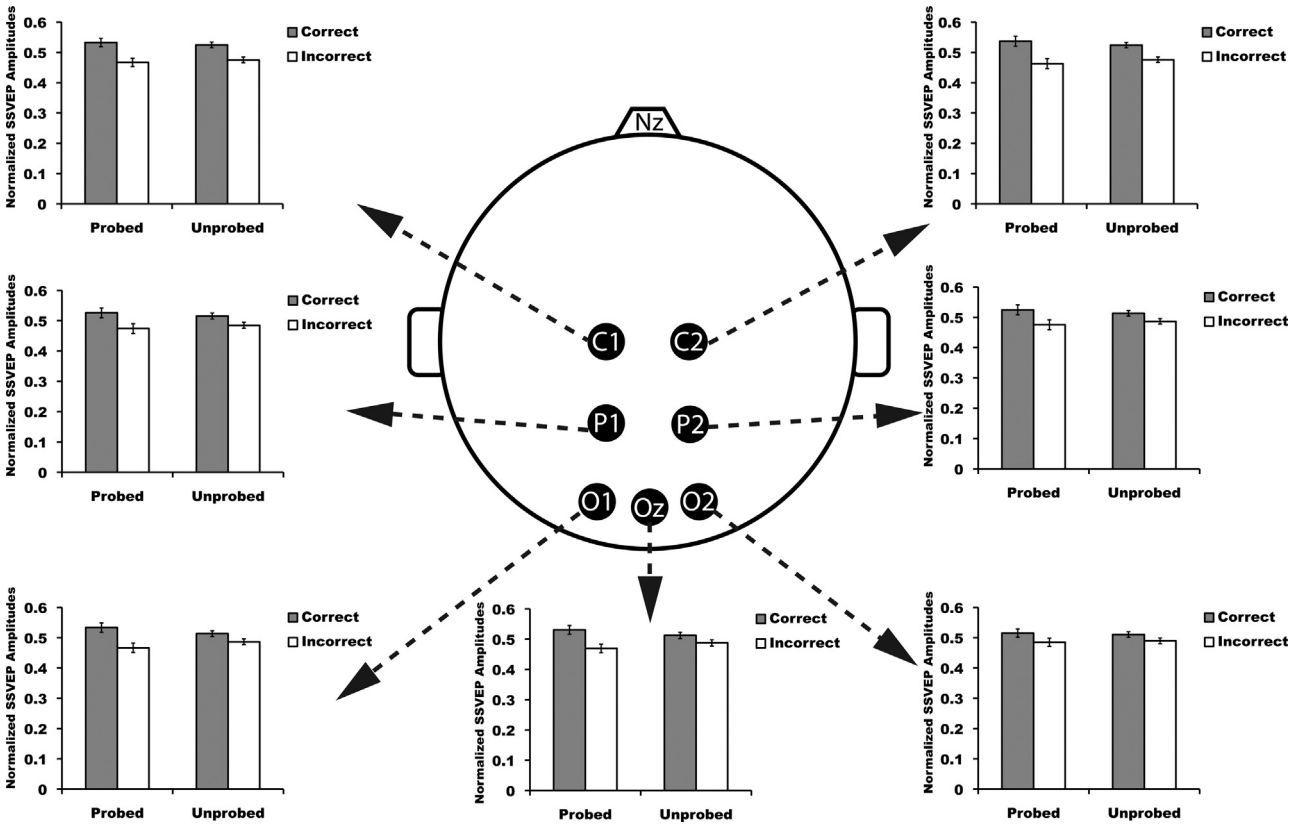

Fig. 5. SSVEP amplitudes as a function of accuracy and probe status at each electrode. SSVEP amplitudes for the fundamental frequencies (2f) computed from the steady-state visual evoked potentials corresponding to electrode sites O1, O2, Oz, P1, P2, C1, and C2. The *y*-axes indicate the mean normalized SSVEP amplitudes for the second harmonics (2f). Error bars represent the standard errors of the means.

The corresponding ANOVA revealed a significant main effect of accuracy ($F(1,22)=12.03$, $MSE=0.32$, $p=0.002$, $\eta_p^2=0.35$). As before, there were no other main effects or interactions between any of the three factors. The main effect of accuracy indicates that during VWM encoding, the SSVEP amplitudes for all items, probed and unprobed, were greater when they were successfully retrieved from VWM than when they were forgotten. Moreover, the lack of a significant interaction between accuracy and probe status demonstrates that the same basic pattern of accuracy observed for the probed items was also observed for the unprobed items.

4. Discussion

In the current study we investigated neural activity at the time of VWM encoding. Specifically, we used a novel approach to measure the neural signatures associated with individual items presented during a VWM task. Each stimulus was flickered at a unique temporal frequency making it possible to examine neural activity in response to each individual item during VWM encoding. This was accomplished by analyzing the amplitude spectra associated with steady-state visual evoked potentials (SSVEPs). SSVEP amplitudes at the time of encoding were significantly larger for items that were successfully retrieved from VWM than for those that were forgotten. Although the statistical significance of this finding was limited to the second harmonic, we note that the same overall pattern of results was observed for the fundamental frequency albeit at a slightly less significant level.

One hypothesis for why this is the case was our use of contrast reversing stimuli. As such, in the current work, the contrast reversals offer the benefit of minimizing potential afterimages during the maintenance phase of the task, but likely lead to an attenuation of the corresponding fundamental frequencies in the recorded EEG. Second, it may be that the perceptual and cognitive processes underlying VWM encoding operate preferentially on contrast-rectified representations of the stimuli (at least in the context of the stimuli as presented in our task). Indeed, several recent studies have analyzed the second harmonic frequency when using the SSVEP technique concurrent with contrast-reversed stimuli (e.g., black–white pattern reversal, Garcia, Srinivasan, & Serences, 2013; Kim, Grabowecky, Paller, & Suzuki, 2011). In addition, Kim and colleagues (2011) recently found evidence suggesting that visual-spatial attention modulates the second, but not first, harmonic frequency of the SSVEP signal. This evidence supports the notion that the second harmonic signal is associated with neural populations that operate on contrast-rectified representations of the stimuli. Our data would suggest that encoding related processes are embodied, at least in part, in such neural populations. The basic finding of increased power for correct relative to incorrect trials observed during encoding suggests that the capacity limitation of VWM is mediated in part by encoding-stage processes. This makes intuitive sense: if an item is not successfully encoded into VWM, it cannot be successfully maintained and ultimately retrieved.

This observation opened the door to testing distinct hypotheses for how capacity limitations at encoding may arise. The results supported the diffuse-resource hypothesis that posits participants, when left to their own devices, will attempt to encode all items present in an array. Their ability to successfully do so and subsequently maintain and remember a probed item depends on the allocation of neural resources deployed during encoding. On a trial-to-trial basis, the amount of resources deployed may vary for a variety of reasons and thus on trials in which fewer resources

were deployed, the participant will be less likely to successfully encode the items in the array. The diffuse-resource hypothesis is consistent with recent behavioral reports of so-called full and partial "lapses" (Mance, Adam, Fukuda, & Vogel, 2014). Full and partial lapses are revealed in full report recall paradigms and describe trials in which participants fail to retrieve any of the items from VWM. These lapses can account for individual differences in overall VWM capacity. Our data would suggest that these lapses might be occurring at the time of encoding rather than later phases of the VWM process; however, future SSVEP studies will need to use a recall paradigm to confirm that this is the case.

Intriguingly, these accuracy dependent modulations of the evoked potential are not readily observable in the time-domain, with correct and incorrect trials producing nearly identical onset VEPs. Moreover, the same overall pattern of results was obtained when the frequency domain analysis was restricted to the final 750 ms of the encoding period, omitting any contribution from the transient onset of the stimulus array (see Supplemental material). Indeed, when limited to the final 750 ms, the main effect of accuracy was statistically significant even for the fundamental frequencies. This suggests that the relatively low frequency power of the onset VEP may have been obscuring accuracy modulations at the fundamental frequencies in the full 1000 ms analysis described above. These additional observations suggest our results represent an index of ongoing encoding related processes that operate while the stimuli are on the screen and are not representative of a pre-stimulus state of the observer (i.e., generalized readiness or arousal).

We note that SSVEPs have been used in previous studies to probe VWM (Ellis, Silberstein, & Nathan, 2006; Perlstein et al. 2003; Silberstein, Nunez, Pipingas, Harris, & Danieli, 2001). In these studies participants performed VWM tasks while a task-irrelevant background stimulus was flickered at a single frequency. This flickering stimulus elicits the SSVEP, the amplitude of which during the maintenance-phase of a VWM task is modulated as a function of VWM load. Similar to those presented here, these past findings demonstrate the effectiveness of using the SSVEP to index the capacity limitation of VWM.

However, the approach we employed here differs from these past SSVEP investigations of VWM in several important respects. First and foremost, the SSVEPs presented here were elicited by individual items in the VWM displays rather than by a task-irrelevant stimulus. This is important because it allowed us to examine the unique SSVEP produced in response to each individual item, rather than an indirect measure of the aggregate processing of the entire memory array. In doing so, we were not only able to examine modulations in the SSVEP as a function of correct and incorrect trials, but to do so for both probed and unprobed items. Second, we examined the SSVEP amplitudes corresponding to the presentation of each individual item during the encoding period of a VWM task. Examining SSVEPs or any neuronally correlated activity during maintenance is no doubt important for examining the overall capacity limitation of VWM. However, the data presented here suggest that observations of capacity limitations observed during the maintenance phase may be in part manifestations of failures that originate during encoding. Future work will obviously be necessary to fully characterize and dissociate sources of capacity limitations that arise during the distinct stages of VWM.

Thus far we have discussed the results in terms of the deployment of neural resources at the time of encoding without being specific as to what these neural resources might represent. Although the present data do not allow us to provide an empirically derived answer to this question, the most likely case is that these neural resources represent visual attention. Attention plays a critical role in the selection of items during VWM encoding (Caplovitz, Fendrich, & Hughes, 2008; Hughes, Caplovitz, Loucks, & Fendrich, 2012; O'Regan, Deubel, Clark, & Rensink, 2000; Rensink, O'Regan, & Clark, 1997; Simons & Levin, 1997). In addition, attention enhances change detection (Hollingworth, 2004; Irwin & Zelinsky, 2002; Rensink et al., 1997; Scholl, 2000; Wolfe, Reinecke, & Brawn, 2006). Moreover, many studies have demonstrated that the amplitude of visual evoked potentials and SSVEP waveforms can be modulated by attention (Anllo-Vento & Hillyard, 1996; Appelbaum, Wade, Pettet, Vildavski and Norcia, 2008; Appelbaum & Norcia, 2009; Hillyard et al., 1997; Mangun, 1995; Morgan et al., 1996; Müller & Hillyard, 2000). Importantly, within the VWM literature, several experiments have directly examined the influence of attention during VWM encoding (for recent reviews see Gazzaley (2011) and Gazzaley and Nobre (2012)). Findings from several recent experiments indicate that selectively attending to task relevant information during encoding modulates the amplitude of various ERP components and is predictive of subsequent success when retrieving representations from VWM (Murray, Nobre, & Stokes, 2011; Rutman, Clapp, Chadick, & Gazzaley, 2010; Zanto & Gazzaley, 2009). These studies highlight the importance of directing attention to task relevant information during VWM encoding to facilitate successful VWM performance.

Although factors such as explicit attentional guidance, cognitive strategy, or bottom-up saliency could influence how participants allocate their attention during encoding, we did not explicitly direct attention to any particular item or location within the stimulus displays. The locations and frequencies of the probed items were also randomized across trials. Under these circumstances, it is reasonable that participants may have adopted a diffuse-resource approach to VWM encoding. This strategy may change as a function of task demands. For example, future experiments explicitly providing spatial cues might expect to observe higher SSVEP amplitudes for the item in the cued location compared to other items. This pattern of evidence would be consistent with the predictions of the focused-resource hypothesis. The novel SSVEP approach used in the current experiment would be ideal for future investigations that involve explicitly guiding attention toward task relevant features, objects, or locations.

In summary, by examining SSVEPs we are able to infer that when individuals are presented with a set of items in a VWM task, they will likely attempt to encode all of the items and not just a select subset. The ability to do so will depend on the amount of neural resources (i.e., attention) that are deployed at the time of encoding. If insufficient resources are allocated, then a probed item will be more likely to be forgotten than remembered. These findings highlight the important role encoding processes play in mediating the overall capacity limitation of VWM.

Acknowledgments

The authors declare no competing financial interests. This work was funded by NEI R15EY022775 to M.E.B. and G.P.C., NIGMS 1P20GM103650-01 to Michael Webster (PI), M.E.B. and G.P.C. (project leaders), and generous startup funds provided by the University of Nevada. The content is solely the responsibility of the authors and does not necessarily represent the official views of the NIH, NIGMS or NEI. We would like to thank Dr. Don L. Jewett for his generous support of this project.

Appendix A. Supplementary material

Supplementary data associated with this article can be found in the online version at http://dx.doi.org/10.1016/j.neuropsychologia.2014.08.020.

References

Albers, A. M., Kok, P., Toni, I., Dijkerman, H. C., & de Lange, F. P. (2013). Shared representations for working memory and mental imagery in early visual cortex. *Current Biology*, *23*(15), 1427–1431.

Alvarez, G. A., & Cavanagh, P. (2004). The capacity of visual short-term memory is set both by visual information load and by number of objects. *Psychological Science*, *15*(2), 106–111.

Anderson, D. E., Vogel, E. K., & Awh, E. (2011). Precision in visual working memory reaches a stable plateau when individual item limits are exceeded. *Journal of Neuroscience*, *31*(3), 1128–1138.

Anllo-Vento, L., & Hillyard, S. A. (1996). Selective attention to the color and direction of moving stimuli: electrophysiological correlates of hierarchical feature selection. *Perception and Psychophysics*, *58*(2), 191–206.

Appelbaum, L. G., & Norcia, A. M. (2009). Attentive and pre-attentive aspects of figural processing. *Journal of Vision*, *9*(11), 1–12.

Appelbaum, L. G., Wade, A. R., Pettet, M. W., Vildavski, V. Y., & Norcia, A. M. (2008). Figure-ground interactions in the human visual cortex. *Journal of Vision*, *8*(9), 1–19.

Awh, E., Barton, B., & Vogel, E. K. (2007). Visual working memory represents a fixed number of items regardless of complexity. *Psychological Science*, *18*(7), 622–628.

Awh, E., & Jonides, J. (2001). Overlapping mechanisms of attention and spatial working memory. *Trends in Cognitive Sciences*, *5*(3), 119–126.

Bays, P. M., Catalao, R. F., & Husain, M. (2009). The precision of visual working memory is set by allocation of a shared resource. *Journal of Vision*, *9*(10), 7 1–11.

Bays, P. M., & Husain, M. (2008). Dynamic shifts of limited working memory resources in human vision. *Science*, *321*(5890), 851–854.

Berryhill, M. E., & Olson, I. R. (2008). Is the posterior parietal lobe involved in working memory retrieval? Evidence from patients with bilateral parietal lobe damage. *Neuropsychologia*, *46*(7), 1775–1786.

Brainard, D. H. (1997). The psychophysics toolbox. *Spatial Vision*, *10*(4), 433–436.

Caplovitz, G. P., Fendrich, R., & Hughes, H. C. (2008). Failures to see: attentive blank stares revealed by change blindness. *Consciousness and Cognition*, *17*(3), 877–886.

Cohen, J. R., Sreenivasan, K. K., & D'Esposito, M. (2012). Correspondence between stimulus encoding- and maintenance-related neural processes underlies successful working memory. *Cerebral Cortex*, *24*, 593–599.

Cowan, N. (2001). The magical number 4 in short-term memory: a reconsideration of mental storage capacity. *Behavioral and Brain Sciences*, *24*(1), 87–114 (discussion 114-185).

D'Esposito, M. (2007). From cognitive to neural models of working memory. *Philosophical Transactions of the Royal Society of London: B Biological Sciences*, *362*(1481), 761–772.

Ellis, K. A., Silberstein, R. B., & Nathan, P. J. (2006). Exploring the temporal dynamics of the spatial working memory n-back task using steady state visual evoked potentials (SSVEP). *Neuroimage*, *31*(4), 1741–1751.

Emrich, S. M., Riggall, A. C., LaRocque, J. J., & Postle, B. R. (2013). Distributed patterns of activity in sensory cortex reflect the precision of multiple items maintained in visual short-term memory. *Journal of Neuroscience*, *33*(15), 6516–6523.

Ester, E. F., Anderson, D. E., Serences, J. T., & Awh, E. (2013). A neural measure of precision in visual working memory. *Journal of Cognitive Neuroscience*, *25*(5), 754–761.

Ester, E. F., Serences, J. T., & Awh, E. (2009). Spatially global representations in human primary visual cortex during working memory maintenance. *Journal of Neuroscience*, *29*(48), 15258–15265.

Fukuda, K., Awh, E., & Vogel, E. K. (2010). Discrete capacity limits in visual working memory. *Current Opinion in Neurobiology*, *20*(2), 177–182.

Funahashi, S., Bruce, C. J., & Goldman-Rakic, P. S. (1990). Visuospatial coding in primate prefrontal neurons revealed by oculomotor paradigms. *Journal of Neurophysiology*, *63*(4), 814–831.

Fuster, J. M., & Alexander, G. E. (1971). Neuron activity related to short-term memory. *Science*, *173*(3997), 652–654.

Fuster, J. M., Bauer, R. H., & Jervey, J. P. (1985). Functional interactions between inferotemporal and prefrontal cortex in a cognitive task. *Brain Research*, *330*(2), 299–307.

Garcia, J. O., Srinivasan, R., & Serences, J. T. (2013). Near-real-time feature-selective modulations in human cortex. *Current Biology*, *23*(6), 515–522.

Gazzaley, A. (2011). Influence of early attentional modulation on working memory. *Neuropsychologia*, *49*(6), 1410–1424.

Gazzaley, A., & Nobre, A. C. (2012). Top-down modulation: bridging selective attention and working memory. *Trends in Cognitive Sciences*, *16*(2), 129–135.

Gazzaley, A., Rissman, J., & D'Esposito, M. (2004). Functional connectivity during working memory maintenance. *Cognitive, Affective, and Behavioral Neuroscience*, *4*(4), 580–599.

Harrison, S. A., & Tong, F. (2009). Decoding reveals the contents of visual working memory in early visual areas. *Nature*, *458*(7238), 632–635.

Hillyard, S. A., Hinrichs, H., Tempelmann, C., Morgan, S. T., Hansen, J. C., Scheich, H., et al. (1997). Combining steady-state visual evoked potentials and f MRI to localize brain activity during selective attention. *Human Brain Mapping*, *5*(4), 287–292.

Hollingworth, A. (2004). Constructing visual representations of natural scenes: the roles of short- and long-term visual memory. *The Journal of Experimental Psychology: Human Perception and Performance*, *30*(3), 519–537.

Hughes, H. C., Caplovitz, G. P., Loucks, R. A., & Fendrich, R. (2012). Attentive and pre-attentive processes in change detection and identification. *PLoS ONE*, *7*(8), e42851.

Irwin, D. E., & Zelinsky, G. J. (2002). Eye movements and scene perception: memory for things observed. *Perception and Psychophysics*, *64*(6), 882–895.

Jasper, H. H. (1958). The ten-twenty electrode system of the International Federation. *Electroencephalography and Clinical Neurophysiology*, *10*, 371–375.

Jiang, Y., Olson, I. R., & Chun, M. M. (2000). Organization of visual short-term memory. *Journal of Experimental Psychology Learning Memory and Cognition*, *26*(3), 683–702.

Kim, Y. J., Grabowecky, M., Paller, K. A., & Suzuki, S. (2011). Differential roles of frequency-following and frequency-doubling visual responses revealed by evoked neural harmonics. *Journal of Cognitive Neuroscience*, *23*(8), 1875–1886.

Klem, G. H., Luders, H. O., Jasper, H. H., & Elger, C. (1999). The ten-twenty electrode system of the International Federation. The International Federation of Clinical Neurophysiology. *Electroencephalography and Clinical Neurophysiology Supplement*, *52*, 3–6.

Luck, S. J., & Vogel, E. K. (2013). Visual working memory capacity: from psychophysics and neurobiology to individual differences. *Trends in Cognitive Sciences*, *17*(8), 391–400.

Magen, H., Emmanouil, T. A., McMains, S. A., Kastner, S., & Treisman, A. (2009). Attentional demands predict short-term memory load response in posterior parietal cortex. *Neuropsychologia*, *47*(8–9), 1790–1798.

Mance, I., Adam, K., Fukuda, K., & Vogel, E. K. (2014). The contribution of attentional lapses to estimates of individual differences in working memory capacity. In: *Proceedings of the Vision Sciences Society Conference.*

Mangun, G. R. (1995). Neural mechanisms of visual selective attention. *Psychophysiology*, *32*(1), 4–18.

McIntosh, A. R., Grady, C. L., Haxby, J. V., Ungerleider, L. G., & Horwitz, B. (1996). Changes in limbic and prefrontal functional interactions in a working memory task for faces. *Cerebral Cortex*, *6*(4), 571–584.

Melcher, D., & Piazza, M. (2011). The role of attentional priority and saliency in determining capacity limits in enumeration and visual working memory. *PLoS ONE*, *6*(12), e29296.

Morgan, S. T., Hansen, J. C., & Hillyard, S. A. (1996). Selective attention to stimulus location modulates the steady-state visual evoked potential. *The Proceedings of the National Academy of Sciences of the United States of America*, *93*(10), 4770–4774.

Müller, M. M., & Hillyard, S. (2000). Concurrent recording of steady-state and transient event-related potentials as indices of visual-spatial selective attention. *Clinical Neurophysiology*, *111*(9), 1544–1552.

Muller, M. M., & Hubner, R. (2002). Can the spotlight of attention be shaped like a doughnut? Evidence from steady-state visual evoked potentials. *Psychological Science*, *13*(2), 119–124.

Muller, M. M., Picton, T. W., Valdes-Sosa, P., Riera, J., Teder-Salejarvi, W. A., & Hillyard, S. A. (1998). Effects of spatial selective attention on the steady-state visual evoked potential in the 20–28 Hz range. *Brain Research Cognitive Brain Research*, *6*(4), 249–261.

Murray, A. M., Nobre, A. C., & Stokes, M. G. (2011). Markers of preparatory attention predict visual short-term memory performance. *Neuropsychologia*, *49*(6), 1458–1465.

O'Regan, J. K., Deubel, H., Clark, J. J., & Rensink, R. A. (2000). Picture changes during blinks: looking without seeing and seeing without looking. *Visual Cognition*, *7*, 191–212.

Offen, S., Schuppeck, D., & Heeger, D. J. (2009). The role of early visual cortex in visual short-term memory and visual attention. *Vision Research*, *49*(10), 1352–1362.

Pelli, D. G. (1997). The VideoToolbox software for visual psychophysics: transforming numbers into movies. *Spatial Vision*, *10*(4), 437–442.

Perlstein, W. M., Cole, M. A., Larson, M., Kelly, K., Seignourel, P., & Keil, A. (2003). Steady-state visual evoked potentials reveal frontally-mediated working memory activity in humans. *Neuroscience Letters*, *342*(3), 191–195.

Postle, B. R. (2006). Working memory as an emergent property of the mind and brain. *Neuroscience*, *139*(1), 23–38.

Regan, D. (1989). *Human brain electrophysiology: evoked potentials and evoked magnetic fields in science and medicine*. New York: Elsevier.

Rensink, R. A., O'Regan, J. K., & Clark, J. J. (1997). To see or not to see: the need for attention to perceive changes in scenes. *Psychological Science*, *8*, 368–373.

Riggall, A. C., & Postle, B. R. (2012). The relationship between working memory storage and elevated activity as measured with functional magnetic resonance imaging. *Journal of Neuroscience*, *32*(38), 12990–12998.

Rutman, A. M., Clapp, W. C., Chadick, J. Z., & Gazzaley, A. (2010). Early top-down control of visual processing predicts working memory performance. *Journal of Cognitive Neuroscience*, *22*(6), 1224–1234.

Scholl, B. J. (2000). Attenuated change blindness for exogenously attended items in a flicker paradigm. *Visual Cognition*, *7*, 377–396.

Serences, J. T., Ester, E. F., Vogel, E. K., & Awh, E. (2009). Stimulus-specific delay activity in human primary visual cortex. *Psychological Science*, *20*(2), 207–214.

Silberstein, R. B., Nunez, P. L., Pipingas, A., Harris, P., & Danieli, F. (2001). Steady state visually evoked potential (SSVEP) topography in a graded working memory task. *The International Journal of Psychophysiology*, *42*(2), 219–232.

Simons, D. J., & Levin, D. T. (1997). Change blindness. *Trends in Cognitive Sciences* *1*(7), 261–267.

Sneve, M. H., Alnaes, D., Endestad, T., Greenlee, M. W., & Magnussen, S. (2012). Visual short-term memory: activity supporting encoding and maintenance in retinotopic visual cortex. *Neuroimage*, *63*(1), 166–178.
Todd, J. J., & Marois, R. (2004). Capacity limit of visual short-term memory in human posterior parietal cortex. *Nature*, *428*(6984), 751–754.
Todd, J. J., & Marois, R. (2005). Posterior parietal cortex activity predicts individual differences in visual short-term memory capacity. *Cognitive, Affective, and Behavioral Neuroscience*, *5*(2), 144–155.
Vogel, E. K., & Machizawa, M. G. (2004). Neural activity predicts individual differences in visual working memory capacity. *Nature*, *428*(6984), 748–751.
Vogel, E. K., McCollough, A. W., & Machizawa, M. G. (2005). Neural measures reveal individual differences in controlling access to working memory. *Nature*, *438* (7067), 500–503.
Wolfe, J., Reinecke, A., & Brawn, P. (2006). Why don't we see changes? The role of attentional bottlenecks and limited visual memory. *Visual Cognition*, *14*, 749–780.
Xu, Y., & Chun, M. M. (2006). Dissociable neural mechanisms supporting visual short-term memory for objects. *Nature*, *440*(7080), 91–95.
Zanto, T. P., & Gazzaley, A. (2009). Neural suppression of irrelevant information underlies optimal working memory performance. *Journal of Neuroscience*, *29* (10), 3059–3066.